**Differential fracture response to traumatic brain injury suggests dominance of neuroinflammatory response in polytrauma**

**Keywords**
Fracture, Traumatic Brain Injury, Polytrauma

Kazuhito Morioka[1,2], Yotvat Marmor[2], Jeffrey A. Sacramento[1], Amity Lin[1], Tiffany Shao[2], Katherine R. Miclau[2], Dan Clark[2], Michael S. Beattie[1], Ralph S Marcucio[2], Theodore Miclau III[2], Adam R. Ferguson[1,3], Jacqueline C. Bresnahan[1*], Chelsea S. Bahney[2,4*]

**Affiliations**
[1]Weill Institute for Neurosciences, Brain and Spinal Injury Center (BASIC), Department of Neurological Surgery, University of California, San Francisco (UCSF) & Zuckerberg San Francisco General Hospital (ZSFG)
1001 Potrero Avenue, Building 1, Room 101, San Francisco, CA 94110, USA

[2]Orthopaedic Trauma Institute, Department of Orthopaedic Surgery, University of California, San Francisco (UCSF) & Zuckerberg San Francisco General Hospital (ZSFG), CA, United States
2550 23rd Street, Building 9, 3rd Floor, San Francisco, CA 94110, USA

[3]San Francisco Veterans Affairs Medical Center, CA, United States
4150 Clement Street, Building 13, Room 114M, San Francisco, CA 94121, USA

[4]Steadman Philippon Research Institute (SPRI)
181 W Meadows Drive, Suite 1000
Vail, CO 81657 USA

**Contributions**
K.M., M.S.B, A.R.F., R.S.M., T.M., J.C.B. and C.S.B. designed the experiments; K.M., Y.M., J.A.S., A.L., T.S., D.C, and C.S.B. executed the experiments; K.M., Y.M., J.A.S., A.L., T.S., K.R.M., D.C. and C.S.B. performed analysis of data; K.M., C.S.B and A.R.F. curated the data, and designed and implemented the analysis; M.S.B., A.R.F., R.S.M., T.M., J.C.B., and C.S.B. provided financial support and materials for the studies; K.M., A.R.F., J.C.B. and C.S.B. wrote and edited the manuscript, with comments from all authors.

**Corresponding authors**
Correspondence to Chelsea S. Bahney (cbahney@sprivail.org) and Jacqueline C. Bresnahan (Jacqueline.Bresnahan@ucsf.edu).

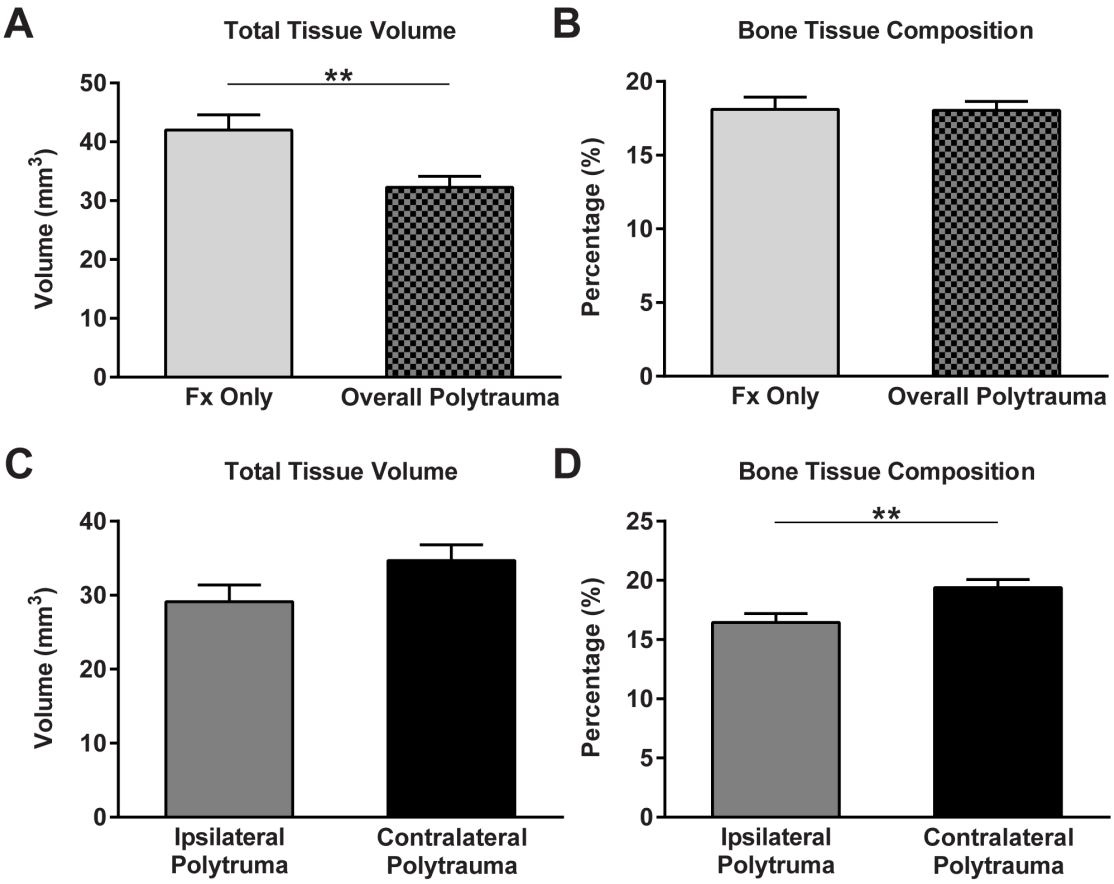


**Supplementary Figure 1. Synthetic effects of traumatic brain injury on fracture healing. (A)** Total volume of the fracture callus and **(B)** bone composition in the fracture callus between the fracture only group (n=17) and the overall polytrauma group (total n=32; the ipsilateral polytrauma group, n=15, plus the contralateral polytrauma group, n=17) during days 5-14 post-injury. The main effect of two-way ANOVA revealed statistically significant effect of traumatic brain injury on total volume of the fracture callus ($F_{(1, 43)} = 9.283$, $p = 0.004$, , $\eta^2 = 0.178$, power = 0.846). **(C)** Total volume of the fracture callus and **(D)** bone composition in the fracture callus between the ipsilateral polytrauma group (n=15) and the contralateral polytrauma group (n=17) during days 5-14 post-injury. The main effect of two-way ANOVA revealed statistically significant lateral effect of traumatic brain injury on bone composition in the fracture callus ($F_{(1, 26)} = 8.297$, $p = 0.008$, $\eta^2 = 0.242$, power = 0.792). The bar graph represents the mean ± standard error of the mean. * = $p \leq 0.05$, ** = $p \leq 0.01$, *** = $p \leq 0.001$.

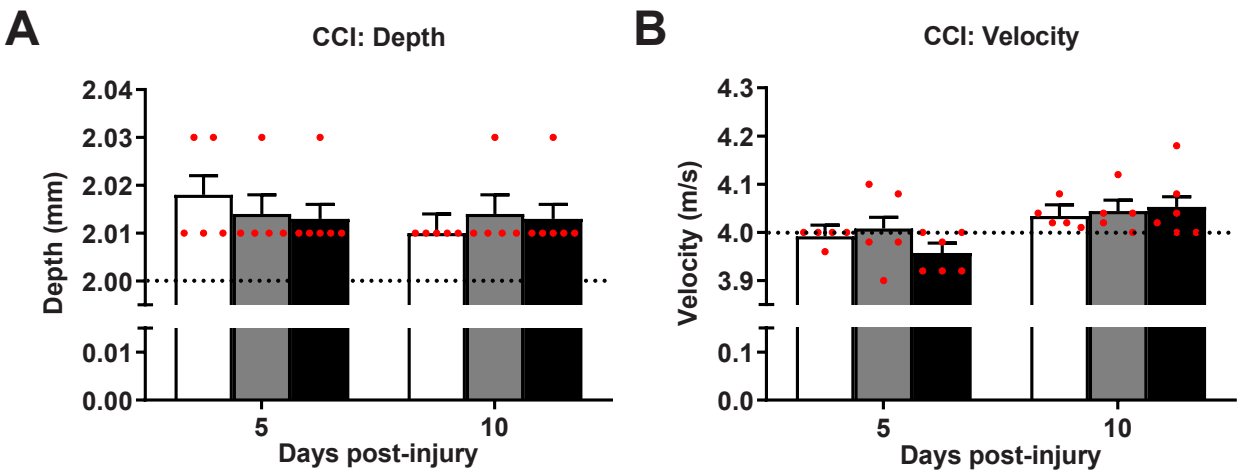


**Supplementary Figure 2. The biomechanical conditions of traumatic brain injury.** The cortical contusion injury was generated using a controlled cortical contusion impactor (CCI) with a depth setting of 2.0 mm, a dwell time of 150 ms, and a velocity of 4 m/s. These input settings are represented by a horizontal dotted line. Actual **(A)** depth and **(B)** velocity recordings from each subject support that the animals received a similar initial impact ($P > 0.05$).

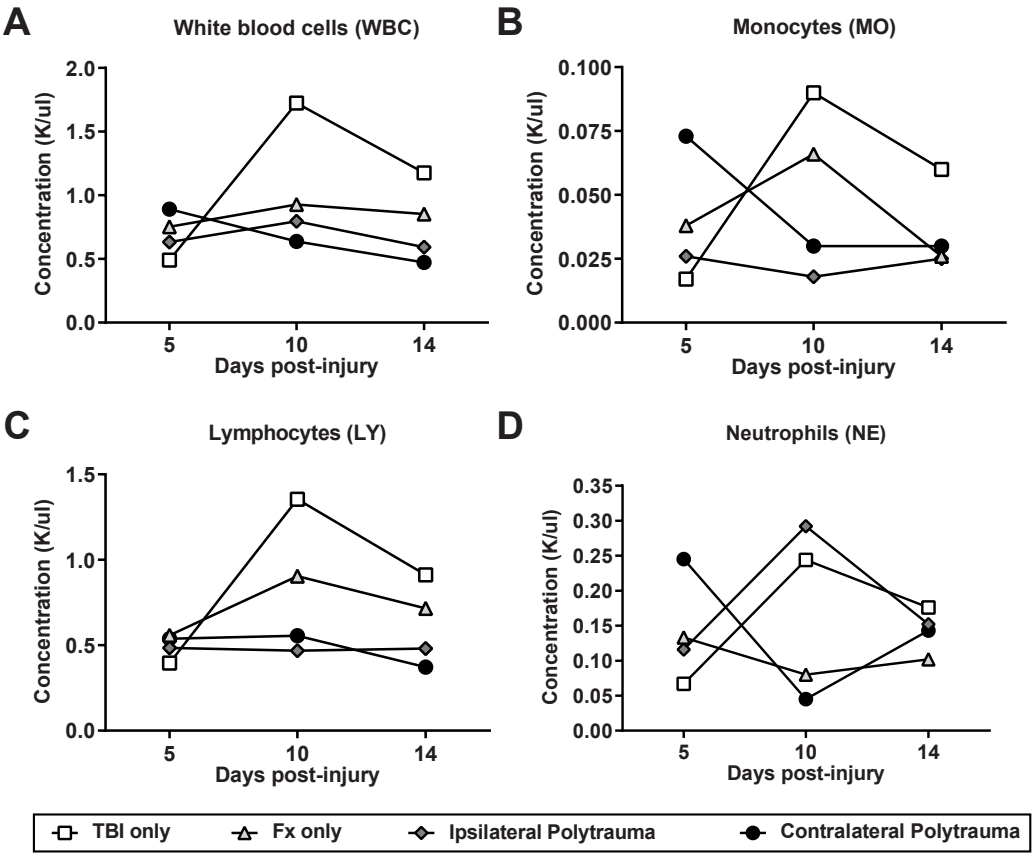


**Supplemental Figure 3. White blood cell differentiation over time**. **(A)** White blood cells **(B)** Neutrophils, **(C)** Lymphocytes, **(D)** Monocytes was quantified at 5, 10 and 14 days post-injury in each group.

A

| Principal Component | Eigenvalues | | | Extraction Sums of Squared Loadings | | |
|---|---|---|---|---|---|---|
| | Total | % of Variance | Cumulative % | Total | % of Variance | Cumulative % |
| 1 | 8.12 | 28.00 | 28.00 | 8.12 | 28.00 | 28.00 |
| 2 | 5.03 | 17.33 | 45.33 | 5.03 | 17.33 | 45.33 |
| 3 | 3.84 | 13.25 | 58.58 | 3.84 | 13.25 | 58.58 |
| 4 | 2.57 | 8.87 | 67.46 | 2.57 | 8.87 | 67.46 |
| 5 | 2.45 | 8.46 | 75.92 | 2.45 | 8.46 | 75.92 |
| 6 | 1.63 | 5.63 | 81.55 | 1.63 | 5.63 | 81.55 |
| 7 | 1.42 | 4.88 | 86.43 | 1.42 | 4.88 | 86.43 |
| 8 | 0.88 | 3.04 | 89.47 | | | |
| 9 | 0.69 | 2.36 | 91.83 | | | |
| 10 | 0.57 | 1.95 | 93.78 | | | |

B

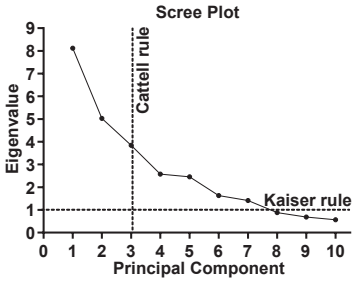


C

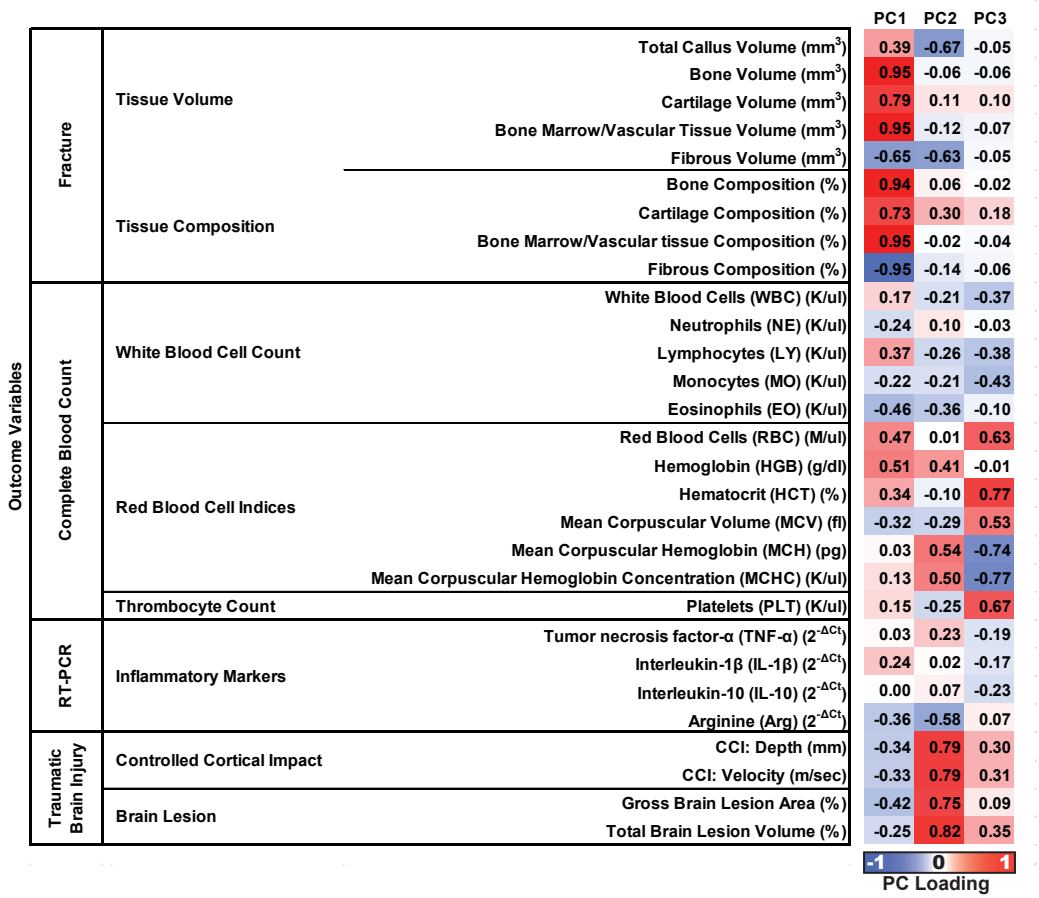


**Supplementary Figure 4. Multivariate analysis of principal component solution. (A)** PCA identified 7 PCs that were accepted using the eigenvalues greater than 1 as the Kaiser criterion. **(B)** The Cattell's Scree test suggested retaining PC1-3 for interpretation of PC content based on significant PC loading values. **(C)** PC over-determination criterion confirmed retaining PC1-3 with loading values above |0.6| in more than 5 outcome variables for the interpretation. PC loading is represented by heat (blue reflects negative and red reflects positive relationship between the individual variable and the loading value).